Volume 1 | Number 1 | Jan 2013 | Pages 1–100

ChemComm

Chemical Communications
www.rsc.org/chemcomm

ROYAL SOCIETY OF CHEMISTRY

This is an *Accepted Manuscript*, which has been through the Royal Society of Chemistry peer review process and has been accepted for publication.

Accepted Manuscripts are published online shortly after acceptance, before technical editing, formatting and proof reading. Using this free service, authors can make their results available to the community, in citable form, before we publish the edited article. We will replace this *Accepted Manuscript* with the edited and formatted *Advance Article* as soon as it is available.

You can find more information about *Accepted Manuscripts* in the **Information for Authors**.

Please note that technical editing may introduce minor changes to the text and/or graphics, which may alter content. The journal's standard **Terms & Conditions** and the **Ethical guidelines** still apply. In no event shall the Royal Society of Chemistry be held responsible for any errors or omissions in this *Accepted Manuscript* or any consequences arising from the use of any information it contains.

Journal Name

Synergistic Effect of a Well-Defined Au@Pt Core-Shell Nanostructure toward Photocatalytic Hydrogen Generation: Interface Engineering to Improve Schottky Barrierand Hydrogen-Evolved Kinetics

Sung-Fu Hung,[a,†] Ya-Chu Yu,[a,†] Nian-Tzu Suen,[a] Guan-QuanTzeng,[a] Ching-Wei Tung,[a] Ying-YaHsu,[a,b] Chia-ShuoHsu,[a] Chung-Kai Chang,[c] Ting-Shan Chan,[c] Hwo-Shuenn Sheu,[c] Jyh-Fu Lee,[c] Hao Ming Chen[a,*]

A well-defined co-catalyst system TiO_2 nanotubes-Au (core)-Pt (shell) was demonstrated as the combination of localized surface plasmon effect of gold and excellent nature of proton reduction of platinum. Furthermore, surface engineering by the descending Fermi energies of gold and platinum was benificial to electron transfer.

Solar energy has been considered as a non-exhausted and renewable resource to satisfy the increasing needs of the energy for modern society. In order to utilize solar energy more efficiently, numerous groups have devoted to develop a technology aiming to convert the solar energy into electricity and/or chemical energy (fuel) such as solar cell, solar water splitting, carbon dioxide reduction and so on.[1-4] Among these technologies, solar water splitting has received many attentionsand production of oxygen and hydrogen gases through either photoelectrochemical approach or electrolysis of water are substantially attractive owing to their critical roles for living beings, especially for hydrogen which possesses high energy density and can be converted into electricity for further utilization.[5-7] As a result, it is highly desirable to design an efficient photocatalytic system to overcome this challenge and meet the requirement of our future daily life.

Among various catalytic systems, titanium dioxide (TiO_2) is one of the most promising materials for photochemical reactions because of its high stability and environment-friendly nature.[8-12] In terms of solar water splitting, TiO_2 with anatase phase possesses a proper band position that can promote hydrogen evolution reaction (HER), while TiO_2 with rutile phase does not have such function due to the improper band position for HER. However, the catalytic ability of anatase $TiO_2$for hydrogen evolution is still relatively low and results in a sluggish kinetic process of HER owing to a small offset in conduction band relative to proton reduction.[13,14] Although one-dimensional TiO_2 is capable of facilitating charge separation of photocarriers and suppressing their recombination,[15,16] its intrinsic surface nature still limits the photocatalytic performance in HER. Toward this end, nanostructured platinum has been demonstrated to be a potential catalyst for HER owing to its extremely low overpotential for proton reduction, and could be employed to overcome the sluggish kinetics.[17,18] Nonetheless, the junction between metal/semiconductor (Pt/TiO_2) bears a substantial Schottky barrier at the interface and obstructs the electrons transferring through the interface. Accordingly, a perfect co-catalytic system is extremely essential not only to lower the Schottky barrier on the interface of semiconductor/metal but also offer sufficient kinetics for proton reduction at the interface of metal/electrolyte, which allows us to achieve an efficient integration with the photocatalytic system.

Herein, we incorporated an Au-Pt core-shell nanostructure as a co-catalytic system to build TiO_2-Au@Pt system for photocatalytic hydrogen generation (as shown in Fig. 1a). Au can capture light to induce localized surface plasmon resonance (LSPR) effects to induce vacancies on conduction band of semiconductor and therefore lower Schottky barrier upon the interface of metal/semiconductor.[19] Furthermore, LSPR effect can provide a beneficial electric field nearby to facilitate the separation of photo-excited carriers and to enhance the photocatalytic performance.[20,21] In addition to plasmonic gold core, platinumshell was utilized due to its intrinsic nature ofcatalysis and porous architecture with high surface area offered more activesites for HER. Although bimetallic Au-Pt nanoparticle modified TiO_2, which combines the characters of Pt and Au, has been attempted in the photocatalytic application.[22-24] However, it is worthy mentioning that a synergistic effect inpresent well-defined gold-platinum core-shell nanostructure (Au@Pt) is achieved while a sequence of junction from Au to Pt induces an extra

a. Department of Chemistry, National Taiwan University, Taipei 106, Taiwan.
b. Program for Science and Technology of Accelerator Light Source, National Chiao Tung University, Hsinchu 300, Taiwan.
c. National Synchrotron Radiation Research Center, Hsinchu 300, Taiwan.
† These authors contribute equally to this work.

electric field to facilitate electron transport, which cannot be achieved by a random distribution counterpart. Therefore, we designed a 1D TiO_2 nanotubes-Au (core)-Pt (shell) (TiO_2 NTs-Au@Pt nanostructure) system, in which Au@Pt nanostructure was employed to deal with both interfaces of semiconductor/metal and metal/electrolyte for efficient hydrogen evolution.
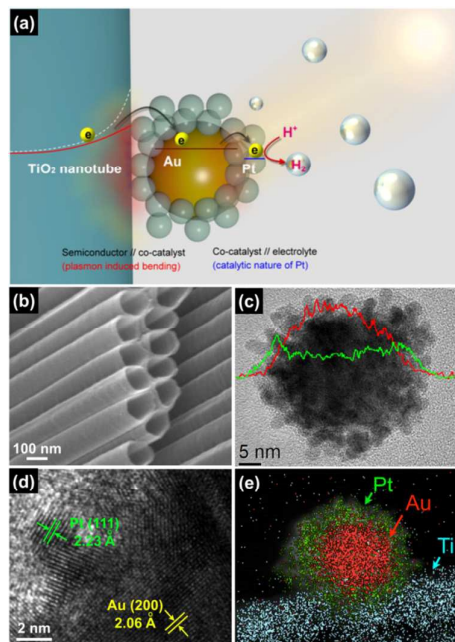

Fig. 1 (a) Schematic illustration of the high-performance photocatalyst for unassisted solar hydrogen evolution.(b) SEM images of TiO_2 nanotubes. (c) Elemental line-scan of Au@Pt nanostructure. (d) High-resolution TEM image and corresponding lattice fringe of Au (200) and Pt (111) planes. (e) Corresponding high-angle annular dark field (HAADF) micrograph and elemental mapping of Ti, Au, and Pt in (e).

One-dimensional TiO_2 nanotubes, as an efficient light harvesting material with high light absorption and scattering, were prepared by electrochemical anodization of titanium foil. The detailed preparation of 1D TiO_2 NTs under various synthetic conditions were investigated and shown in Fig. S1-3. Top view of TiO_2 nanotubes exhibited a uniform shape of nanotube with an inner-diameter around 100 nm, which could provide sufficient space for subsequent deposition of Au@Pt nanostructure (Fig. 1b). Notably, the ultra-thin wall of TiO_2 NTs are beneficial to shorten the route of carriers migrating toward the surface for consecutive reaction.[25] In terms of Au@Pt nanostructure, a soft template of F127 was essential to form a porous structure of Pt-shell (as shown in Fig. 1c**)** and line-scan profile showed a typical core-shell characteristic while higher contents of Au and Pt were present at the core and shell, respectively. The individual lattice fringes of Au and Pt were observed in the high-resolution TEM image (Fig. 1d), twodspacing of 2.06 Å and 2.23 Å were found in the core region and porous region and could be assigned to Au (002) plane and Pt (111) plane, respectively. This observation suggested that an Au@Pt core-shell conformation had been realized in present study. It is worthy saying that this co-reduction synthesis of Au and Pt ions could produce a core-shell nano-architecture and

neither random alloy nor a mixture of individual components was observed. Because of a small lattice mismatch between Au and Pt (~4%), surface-catalytic nucleation upon the surface of Au core considerably facilitated the nucleation of Pt over the Au rather than self-nucleation to produce individual Pt nanoparticles. TEM images of Au@Pt nanostructures prepared by various reaction times and corresponding TiO_2 NTs-Au@Pt nanostructures were shown in Fig. S4-5. By employing 3-mercaptopropionic acid as a linker, the surface of Au@Pt nanostructure could be functionalized with hydroxyl group owing to a strong interaction between Au/Pt and S, which allowed significantly anchoring the Au@Pt nanostructure on the surface of TiO_2 to result in the desired TiO_2 NTs-Au@Pt composite. Scanning TEM image of TiO_2 NTs-Au@Pt composite and high-angle annular dark field (HAADF) image with corresponding elemental mapping of Ti, Au, and Pt were shown in Fig. 1e, indicating that the Au@Pt nanostructure was not varied during the self-assembling process and was successfully integrated upon the TiO_2 NTs.
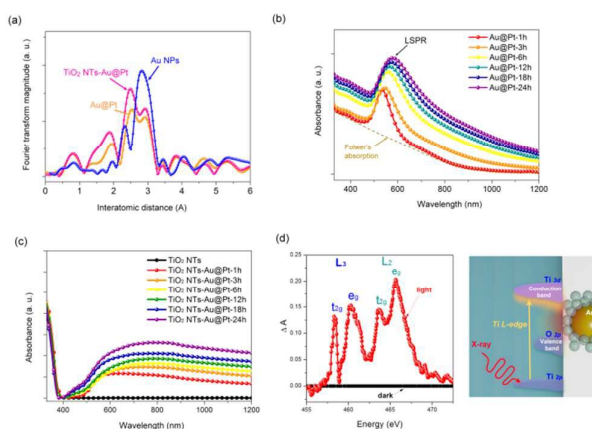

Fig. 2 (a) Fourier transform of Extended X-ray absorption fine structure (EXAFS) spectra of Au L_{III}-edge of Au nanoparticles, Au@Pt, and TiO_2 NTs-Au@Pt samples. (b) Optical properties of Au@Pt nanostructure with various reaction time. (c) UV-Vis absorption spectra of self-assembled TiO_2 NTs-Au@Pt composite with various reaction time. (d) XANES Differential spectra of Ti L_{III}-edge for TiO_2 NTs-Au@Pt nanostructure with/without illumination.

In order to further reveal the atomic distribution of Au and Pt, extended X-ray absorption fine structure (EXAFS) spectra of Au L_{III}-edge were conducted to show that there was an intense peak at a shorter interatomic distance (approximately 2.6 Å) as compared to that of Au nanoparticles (Fig. 2a). This observation could be attributed to a smaller atomic radius of platinum and suggested a significant area of interfaces formed between Au and Pt atoms. The Au L_{III}-edge spectrum of Au@Pt nanostructure was nearly unchanged after self-assembling, which suggested that this method could effectively combine two different constituents without destructing the individual property of Au@Pt (XRD was shown in Fig. S6). Moreover, according to the results of XPS (Fig. S7), close-packed metals caused a strong interaction between Au and Pt atoms in which the binding energies of Au and Pt were augmented as the ratio of Pt increased. This finding indicated that Pt would gain electrons from the Au due to a difference in both

electronegativity and work function,[26,27] and substantially affect both optical and photocatalytic characteristics. Au@Pt nanostructure showed a strong surface plasmon resonance peak composed of a unique absorption peak at ~ 550 nm (Fig. 2b).[28] Notice that the intensities of LSPR absorption peak slightly decreased with increasing content of platinum in Au@Pt nanostructure. In addition, the peak became broader and its position shifted toward longer wavelength region, suggested that Pt shell led to a gradual dampening of LSPR absorption upon Au core.[29-31] Once Au@Pt nanostructure was self-assembled on the surface of TiO_2 NTs, a strong absorption was observed in both visible and near infrared regions (Fig. 2c). This phenomenon may be attributed to either the LSPR absorption of platinum or formation of aggregated colloid platinum that showed a continuous absorption feature like bulk status.[17,32-34] Nevertheless, the former statement could be ruled out since the LSPR absorption of platinum nanoparticles should be located at 200-300 nm while Au@Pt nanostructures seem to lack this obvious occurrence.[34,35] During the process of self-assembling, platinum was seen to contact with TiO_2 and led to aggregation-like behavior of platinum on the surface of TiO_2 NTs. As a result, the aggregated-like platinum caused the large absorption of visible light and could shadow the LSPR absorption of gold. Accordingly, it could be expected that it exists a trade-off effect on the photocatalytic performance.

Plasmon-induced electromagnetic field has been demonstrated to further generate vacancies (states) in the conduction band of ZnO (similar to Zeeman effect), which resulted in a down-shift of the height of conduction band edge and then lowered the Schottky barrier between ZnO and Au to facilitate the charge transfer of photoelectrons.[19] For this end, X-ray absorption spectrum of Ti L_{III}-edge was performed to probe the unoccupied states in the conduction band of TiO_2 which was mainly constituted of 3d band of Ti, and was able to monitor the change in conduction band of TiO_2 since the L_{III} absorption referred to a transition from 2p to 3d band of Ti (Fig. 2d). There was an obvious difference in Ti XANES under illumination, which suggested that extra vacancies (states) were generated in TiO_2 NTs once LSPR effect from Au@Pt nanostructure were launched by illumination. This corroborated a fact that the Schottky barrier between TiO_2 NTs and Pt would be downshifted. In addition to plasmon-induced vacancies over the semiconductor, the electromagnetic field near the plasmonic gold can simultaneously produce a plasmon-induced resonance energy transfer (PIRET) effect to improve the photocatalysis.[26] Plasmonic gold received a radiation of LSPR absorption region and subsequently generated both plasmon-induced vacancies and PIRET effect at the interface of semiconductor/metal, more photoelectrons were produced for facilitating the charge-transfer from TiO_2 to co-catalyst and charge-excitation over TiO_2.

In terms of the interface between metal and electrolyte, a descending Fermi level in Au@Pt nanostructure remarkably constructed an extra electric field to facilitate the electron transporting within metal co-catalyst and migrating toward the electrolyte for chemical reaction (as illustrated in Fig. 1a). Once electrons in Pt transferred to electrolyte for HER, the electrons

in Au would have a driving force with energy of $e\varphi$ to transport toward Pt owing to a higher Fermi level of Au with a potential difference of φ in between (Fig. S8), suggested that the difference of Fermi level between Au and Pt would benefit the photocatalysis. Consequently, the porous Pt nanostructure covering Au core could effectively cope with the interface of metal/electrolyte through both difference of Fermi energy and its excellent nature of proton reduction.
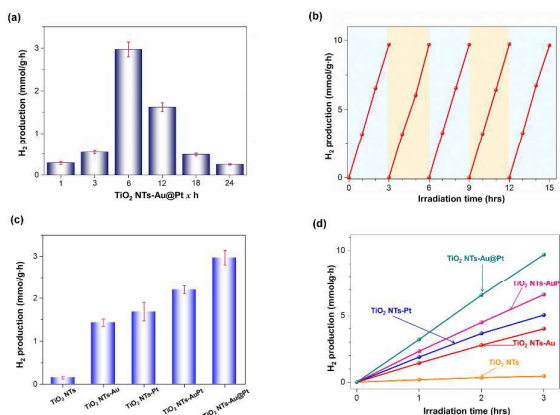

Fig.3 (a) Hydrogen gas evolution of TiO_2 NTs-Au@Pt nanostructure with various Au@Pt reaction periods under solar light irradiation. (b) Time course of H_2 evolution using TiO_2 NTs-Au@Pt-6h in neutral electrolyte under solar light irradiation. (c) H_2 evolution of TiO_2 NTs, TiO_2 NTs-Au, TiO_2 NTs-Pt, TiO_2 NTs-AuPt, and TiO_2 NTs-Au@Pt samples. (d) Time course of H_2 evolution using different photocatalysts.

Practical photocatalytic efficiency of TiO_2 NTs-Au@Pt composite for photocatalytic HER was shown in Fig. 3a, the hydrogen production of Au@Pt-6h sample reached a maximum amount of about 3 mmolg^{-1}h^{-1}, which was ten times higher than that of Au@Pt-1h sample. This occurrence resulted from LSPR effects from gold that could build an electromagnetic field on the surface of TiO_2 NTs to simultaneously assist the charge separation of photocarriers within TiO_2 NTs, lower the Schottky barrier, and launch PIRET mechanism for substantially improving the photocatalysis of present nanostructure. However, once the reaction time of Au@Pt samples exceeded six hours, the feature absorption of platinum presented as well as the elemental analysis showed an increase in platinum amount, this might shadow the light illuminating upon gold and weaken the LSPR effect of gold to restrain the photocatalytic ability. An optimized photocatalytic hydrogen generation could be achieved through a proper Pt/Au ratio, in which both LSPR effect of gold and superior HER activity of platinum could significantly maximize. In addition, the TiO_2 NTs-Au@Pt composite showed an excellent stability for hydrogen generation without noticeable decay in couples of hours and reproducibility in different runs of hydrogen generation (as shown in Fig. 3b).

To further confirm the nature of Au@Pt nanostructure, the hydrogen generation of bare TiO_2 NTs, TiO_2 NTs-Au nanostructures, TiO_2 NTs-Pt nanostructures, and TiO_2 NTs-AuPt (random alloy) were compared with TiO_2 NTs-Au@Pt composite (as shown in Fig. 3c) while the individual TEM images and size statistics of gold, platinum nanoparticles and AuPt random alloy were revealed in Fig. S9-S11. The hydrogen

production was intensely enhanced owing to the assistance of PIRET effect by gold nanoparticles while bare TiO_2 NTs showed relatively poor activity to generate hydrogen gas due to its inferior charge separation. Once TiO_2 NTs were decorated by platinum nanoparticles, the catalytic performance was slightly higher than that of TiO_2 NTs-Au due to remarkable HER catalytic activity. Notably, the hydrogen generation of TiO_2 NTs-Au@Pt composite was twenty times higher than that of bare TiO_2 NTs and superior to that of TiO_2 NTs-Au, TiO_2 NTs-Pt as well as TiO_2 NTs-AuPt, which could be attributed to the synergistic contribution of both plasmonic gold and platinum. Moreover, the photocatalytic activities were conducted in either UV or visible region to specify the LSPR effects, we detected only trace amount of hydrogen gases in each catalyst (Fig. S12). Noted that the hydrogen generation in visible region was much lower than that in UV region and white light, it suggested that the significant enhancement of hydrogen production as a result of hot electrons excited in Au by SPR effect could be ruled out and also confirmed that the enhancement could be attributed to the synergistic effects owing to downshifted Schottky barrier and PIRET effect. To consider the enhancement between UV and white light cases, the TiO_2 NTs-Au@Pt sample could significantly show a better enhancement of photocatalytic activity (2.97/2.05) than that of TiO_2 NTs-AuPt alloy sample (2.18/1.69), which also suggested that core-shell nanostructure was able to offer additional effects for enhancing their charge-separation and photocatalytic activity (Fig. S12). This result could consolidate that an additional electric field induced by the descending potential level between Au/Pt could also benefit the photocatalysis (a photocatalytical enhancement was revealed in $Si-SiO_2-Ti-Pt$ composite system as well).[36] Furthermore, the stability measurement in Fig. 3d showed that TiO_2 NTs-Au@Pt composite could generate hydrogen gas without any significant decay. In contrast, the hydrogen production rates of TiO_2 NTs, TiO_2 NTs-Au, and TiO_2 NTs-Pt samples slightly decreased after long-term use.

In summary, Au@Pt nanostructure modified the photocatalytic performance of TiO_2 NTs and improved the stability of hydrogen production in long-term test. The synergistic nanostructure can not only lower the Schottky barrier on the interface of semiconductor/metal but also achieve sufficient kinetics for proton reduction at the interface of metal/electrolyte, which leads to a significant increase of overall efficiencies and become a promising material for practical applications.

Notes and references

1   I. Chung, B. Lee, J. He, R. P. H. Chang and M. G. Kanatzidis, *Nature*, 2013, **485**, 486–489.
2   M. Grätzel, *Nature*, 2001, **414**, 338–344.
3   A. Kudo and Y. Miseki, *Chem. Soc. Rev.*, 2009, **38**, 253–278.
4   Ş. Neaţu, J. A. Maciá-Agulló, P. Concepción and H. Garcia, *J. Am. Chem. Soc.*, 2014, **136**, 15969–15976.
5   Y. Wang, Y.-Y. Zhang, J. Tang, H. Wu, M. Xu, Z. Peng, X.-G. Gong and G. Zheng, *ACS Nano*, 2013, **7**, 9375–9383.
6   C.-W. Tung, Y.-Y. Hsu, Y.-P. Shen, Y. Zheng, T.-S. Chan, H.-S. Sheu, Y.-C. Cheng and H. M. Chen, *Nat. Commun.*, 2015, **6**, 8106.
7   H.-Y. Wang, Y.-Y. Hsu, R. Chen, T.-S. Chan, H. M. Chen and B. Liu, *Adv. Energy Mater.*, 2015, **5**, 1500091.
8   B. Liu, H. M. Chen, C. Liu, S. C. Andrews, C. Hahn and P. Yang, *J. Am. Chem. Soc.*, 2013, **135**, 9995–9998.
9   A. Fujishima and K. Honda, *Nature*, 1972, **238**, 37–38.
10 L. Duan, L. Wang, F. Li, F. Li and L. Sun, *Acc. Chem. Res.*, 2015, **48**, 2084–2096.
11 H. M. Chen, C. K. Chen, R.-S. Liu, L. Zhang, J. Zhang and D. P. Wilkinson, *Chem. Soc. Rev.*, 2012, **41**, 5654–5671.
12 M. G. Walter, E. L. Warren, J. R. McKone, S. W. Boettcher, Q. Mi, E. A. Santori and N. S. Lewis, *Chem. Rev.*, 2010, **110**, 6446–6473.
13 D. D'Elia, C. Beauger, J.-F. Hochepied, A. Rigacci, M.-H. Berger, N. Keller, V. Keller-Spitzer, Y. Suzuki, J.-C. Valmalette, M. Benabdesselam and P. Achard, *Int. J. Hydrogen Energy*, 2011, **36**, 14360–14373.
14 M. Shen, Z. Yan, L. Yang, P. Du, J. Zhang and Bin Xiang, *Chem. Commun.*, 2014, **50**, 15447–15449.
15 P. Roy, S. Berger and P. Schmuki, *Angew. Chem. Int. Ed.*, 2011, **50**, 2904–2939.
16 F.-X. Xiao, S.-F. Hung, J. Miao, H.-Y. Wang, H. Yang and B. Liu, *Small*, 2014, **11**, 554–567.
17 J. Yu, L. Qi and M. Jaroniec, *J. Phys. Chem. C*, 2010, **114**, 13118–13125.
18 C. Liu, J. Tang, H. M. Chen, B. Liu and P. Yang, *Nano Lett.*, 2013, **13**, 2989–2992.
19 H. M. Chen, C. K. Chen, C.-J. Chen, L.-C. Cheng, P. C. Wu, B. H. Cheng, Y. Z. Ho, M. L. Tseng, Y.-Y. Hsu, T.-S. Chan, J.-F. Lee, R.-S. Liu and D. P. Tsai, *ACS Nano*, 2012, **6**, 7362–7372.
20 J. Li, S. K. Cushing, P. Zheng, F. Meng, D. Chu and N. Wu, *Nat. Commun.*, 2013, **4**, 2651.
21 Y.-C. Pu, G. Wang, K.-D. Chang, Y. Ling, Y.-K. Lin, B. C. Fitzmorris, C.-M. Liu, X. Lu, Y. Tong, J. Z. Zhang, Y.-J. Hsu and Y. Li, *Nano Lett.*, 2013, **13**, 3817–3823.
22 A. Gallo, M. Marelli, R. Psaro, V. Gombac, T. Montini, P. Fornasiero, R. Pievo and V. D. Santo, *Green Chem.*, 2012, **14**, 330–333.
23 A. A. Melvin, K. Illath, T. Das, T. Raja, S. Bhattacharyya and C. S. Gopinath, *Nanoscale*, 2015, **7**, 13477–13488.
24 F. Wang, Y. Jiang, D. J. Lawes, G. E. Ball, C. Zhou, Z. Liu and R. Amal, *ACS Catal.*, 2015, **5**, 3924–3931.
25 K. Lee, A. Mazare and P. Schmuki, *Chem. Rev.*, 2014, **114**, 9385–9454.
26 S. Li, Y. Dong, X. Bi and M. Tang, *Int. J. Electrochem. Sci.*, 2013, **8**, 8662–8668.
27 J. Zeng, J. Yang, J. Y. Lee and W. Zhou, *J. Phys. Chem. B*, 2006, **110**, 24606–24611.
28 P. Zhang, T. Wang and J. Gong, *Adv. Mater.*, 2015, **27**, 5328–5342.
29 B. Du, O. Zaluzhna and Y. J. Tong, *Phys. Chem. Chem. Phys.*, 2011, **13**, 11568–11574.
30 R. H. Fowler, *Phys. Rev.*, 1931, **38**, 45–56.
31 M. W. Knight, H. Sobhani, P. Nordlander and N. J. Halas, *Science*, 2011, **332**, 702–704.
32 R. Bouwman and W. Sachtler, *J. Catal.*, 1970, **19**, 127–139.
33 Y.-C. Yeo, T.-J. King and C. Hu, *J. Appl. Phys.*, 2002, **92**, 7266.
34 S. Jung, K. L. Shuford and S. Park, *J. Phys. Chem. C*, 2011, **115**, 19049–19053.
35 A. Henglein, B. G. Ershov and M. Malow, *J. Phys. Chem.*, 1995, **99**, 14129–14136.
36 D. V. Esposito, *Nat. Mater.*, 2013, **12**, 562–568.